

Binding Energies of Silver Ion–Ligand, L, Complexes AgL_2^+ Determined from Ligand-Exchange Equilibria in the Gas Phase

Haiteng Deng and Paul Kebarle*

Department of Chemistry, University of Alberta, Edmonton, Alberta, Canada T6G 2G2

Received: September 22, 1997; In Final Form: November 13, 1997

The free energy ΔG° , entropy ΔS° , and enthalpy ΔH° for the reaction: $\text{AgL}_2^+ = \text{Ag}^+ + 2\text{L}$ in the gas phase were determined for 16 different ligands L which included oxygen bases such as H_2O , MeOH , EtOH , Me_2CO , and Me_2SO , nitrogen bases NH_3 and MeCN , and sulfur bases Me_2S . The determinations were based on measurements of the exchange equilibria $\text{AgA}_2^+ + \text{B} = \text{AgAB}^+ + \text{A}$ and $\text{AgAB}^+ + \text{B} = \text{AgB}_2^+ + \text{A}$ where A and B are different ligands L. The exchange equilibria were determined in a “high”-pressure ion source at 10 Torr bath gas containing A and B in the 10–100 mTorr range and using $\text{Ag}(\text{MeOH})_2^+$ ions produced by electrospray. A scale of ΔG° values for the exchange reaction $\text{AgA}_2^+ + 2\text{B} = \text{AgB}_2^+ + 2\text{A}$ was established and calibrated to the ΔG° for $\text{Ag}(\text{H}_2\text{O})_2^+ = \text{Ag}^+ + 2\text{H}_2\text{O}$, due to Holland and Castleman, obtaining thus absolute ΔG° values for all ligands involved. Theoretically calculated ΔS° values led to ΔH° . Comparison of the ΔG° and ΔH° results with binding energies for the same ligands in complexes with the alkali ions Li^+ and K^+ showed that while a good correlation is observed for the alkali ions as a group, only a very poor correlation is observed between the alkali ions and Ag^+ . In particular, the “soft” base Me_2S showed, relative to the “hard” oxygen bases, a much stronger bonding to Ag^+ . The comparison was extended to CuL_2^+ on the basis of additional exchange equilibria determinations. The CuL_2^+ and AgL_2^+ results combined with earlier determinations of MnL_2^+ , CoL_2^+ and CuL_2^+ by Jones and Staley provide a partial confirmation of the hard and soft acid–base (HSAB) concept for these systems. However, a more detailed comparison on the basis of the absolute hardness, η , scale developed by Pearson and co-workers indicates only a very limited agreement when a larger variety of bases is included.

Introduction

The chemistry of transition-metal ion–ligand complexes, in solution is an important and well-established field. Studies of the gas-phase properties and particularly the gas-phase thermochemistry of such complexes were initiated more recently; see, for example, refs 1a and 1b,c. The gas-phase studies provide bond energies and reactivities in the absence of the solvent medium, and comparisons with the behavior in solution lead to information on the effect of the solvent. Gas-phase thermochemical data are also of interest because they are directly comparable with thermochemical data obtained by theoretical methods such as ab initio calculations.

The hard and soft acids and bases principle² (HSAB), which was established^{2a,b} on the basis of experimental data in solution, has been expanded more recently to provide quantitative values for the hardness or softness of the acids and bases. This expanded treatment is applicable directly only to gas-phase complexes. Therefore, experimental data for the bonding in gas-phase Lewis acid–base complexes as presented here are also of interest from the standpoint of the HSAB principle.

A new application of gas-phase ion thermochemical data has arisen recently with the advent^{3a,b} of modern analytical mass spectrometric methods such as electrospray (ES) which produces gas-phase ions by transfer of ions from solution to the gas phase.^{3c} Many of the species observed mass spectrometrically are ion–ligand complexes, and the stability of such complexes in the gas phase may be a determining factor whether they will be present and observed in the ES mass spectra.

Thermochemical measurements in the gas phase have been

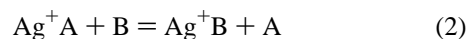
mainly based on gas-phase ion equilibria determinations^{4,5} or collision-induced dissociation threshold energy determinations.^{6,7}

Holland and Castleman⁵ have obtained the free energy, $\Delta G^\circ_{n-1,n}$ and enthalpy changes $\Delta H^\circ_{n-1,n}$ for the reactions



by determining the association equilibria, eq 1, and their temperature dependence, for $\text{L} = (\text{H}_2\text{O}, \text{NH}_3, \text{pyridine})$. However, the range $(n - 1, n)$ for NH_3 and pyridine did not include the important $(0, 1)$ determinations because the bond enthalpies $-\Delta H_{0,1}$ are high for these ligands, and the $(0, 1)$ equilibria would have been observable only at temperatures that were higher than those accessible with the apparatus used ($T < 550 \text{ K}$). Many ligands of interest such as benzene, diethyl ether, acetone, acetonitrile, dimethyl sulfoxide (DMSO), and others are expected to lead to even stronger bonding, which means that their $(0, 1)$ thermochemistry will also not be easily accessible with the ion association equilibria method. The alternative CID threshold method^{6,7} which is not restricted to a low bond energy range has not been applied so far to Ag^+L_n complexes other than for $\text{L} = \text{CO}$ ^{6,7a} and C_6H_6 .^{7b}

An alternative equilibrium method applicable to high bond energy ligands is the ligand exchange method which, for a one-ligand A complex with Ag^+ , can be represented by

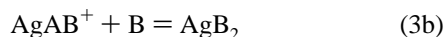


By measuring exchange equilibria eq 2 with progressively stronger bonding ligands A and B, a relative scale of $\Delta G^\circ_{0,1}$ -

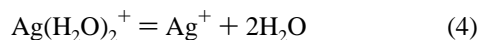
(L) values can be established. This scale can then be converted to absolute values, $\Delta G_{0,1}^{\circ}(L)$, if the value for one ligand is available from other measurements such as ion association equilibria measurements or CID thresholds. This procedure is analogous to the method used for determinations of gas-phase basicities from scales based on proton-transfer equilibria determinations.⁸ Taft et al.⁹ have applied the exchange equilibria approach to lithium ion–ligand complexes, determining in this manner the $\Delta G_{0,1}^{\circ}$ values for some 58 different ligands with progressively stronger bonding. The equilibria determinations of Taft were performed at very low ion source pressures and at ~ 100 °C temperature with an ion cyclotron resonance (ICR) mass spectrometer.

Recently, we developed an apparatus^{10,11} with which ion equilibria can be determined involving ions and ion–molecule complexes produced by electrospray. A great advantage of electrospray is the ease of gas-phase ion production since in general all that is required is to have the ions available in a suitable solution and use this solution in the ES experiment. As was indicated above, ES is a source of many gas-phase ions that cannot be produced by any other means. Important examples are ions of biochemical interest such as polyprotonated peptides and proteins and polydeprotonated nucleic acids and singly and multiply charged alkaline earth and transition-metal ion–ligand complexes. Thus, electrospray provides unique opportunities not only for analytical applications³ but also for physical measurements.^{10–12}

In the present work, silver ion complexes $\text{Ag}(\text{MeOH})_2^+$ were obtained from ES of silver nitrate solutions in methanol (MeOH). These complexes were then converted to other ligand complexes by ion–molecule reactions in a gas-phase reaction chamber.¹¹ The exchange equilibria^{3a,b} were determined for a series of ligands $L = A$ and B .



A scale of $\Delta G_{0,3}^{\circ}$ was obtained and calibrated to the absolute values for the reaction



determined by Holland and Castleman,⁵ obtaining thus absolute values for the reaction



involving the various ligands L used. While these results are restricted to the two-ligand AgL_2^+ complexes, these complexes are of particular interest since they represent the first two very strong bonding interactions in the linear AgL_2^+ complex achieved through $\text{sd}\sigma$ hybridization of the transition-metal ion.^{13,14}

Experimental Section

Because the present determinations are the first measurements of exchange equilibria with the high-pressure reaction chamber,¹¹ a more complete account of measurement procedures and observations is given in sections (b) and (c) of this chapter.

(a) **Apparatus.** The ion source reaction chamber (see Figure 1) has been described previously¹¹ in some detail. Therefore,

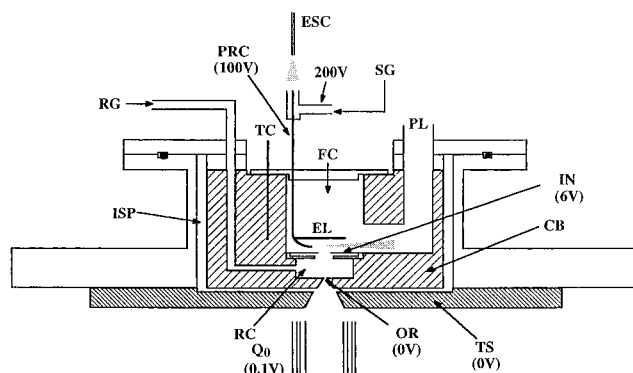


Figure 1. Ion source and reaction chamber for determination of ion–molecule equilibria. Electrospray generator ESC. Pressure reducing capillary PRC transfers ions, produced by electrospray, from atmospheric pressure to 10 Torr pressure of fore chamber FC. Electric field imposed between electrode EL and interface plate IN drifts ions from PRC plume into reaction chamber RC. Reagent gas RG consisting of 10 Torr of N_2 and reactant gases A and B at 1–100 mTorr partial pressures flows into reaction chamber RC and out of RC into fore chamber FC. Gases pumped out of fore chamber by pumping lead PL. Ion–molecule equilibria establish in reaction chamber RC. Ions escaping through orifice OR into vacuum are determined with a quadrupole mass spectrometer. Ion source reaction chamber is machined out of a copper block CB which is heated by heating cartridges (not shown). Temperature of block is determined with thermocouple TC.

only a brief account will be given here. The Ag^+ ions needed in the present work were produced by electrospray from 10^{-4} mol/L solutions of AgNO_3 in methanol. The solution was electrosprayed by passing it at a $2 \mu\text{L}/\text{min}$ flow rate through the electrospray capillary (ESC) (see Figure 1). Some of the spray vapors containing $\text{Ag}(\text{MeOH})_n^+$ ions are transferred to the fore chamber (FC) of the ion source via the capillary (PRC). To reduce solvent vapor intake, the entrance of the capillary (PRC) was purged with source gas (SG), consisting of dry N_2 . The fore chamber (FC) and reaction chamber (RC) were at the same pressure, 10 Torr, which was maintained by pumping via the pumping lead (PL). Ions in the plume at the exit tip of the capillary (PRC) are deflected toward the 4 mm entrance hole in the interface electrode (IN), which leads to the reaction chamber (RC). The ion deflection is achieved by applying an electric field between the electrode attached to PRC and IN. Reagent gas consisting of dry nitrogen N_2 at 10 Torr and the ligand vapor(s) at known partial pressures in the milli-Torr range flow through the lead (RG) into RC and out of RC through the hole in IN. The ions react with ligand molecules L in the reaction chamber (RC). Some of the ions reaching the orifice (OR) at the bottom of the reaction chamber escape into the vacuum region which houses the triple quadrupole mass spectrometer used for ion detection. The ion intensity ratios detected with the quadrupole Q_3 were used for the equilibrium determinations (see eqs 1–4); Q_0 , Q_1 , and Q_2 were used as ion guides (AC only).

The fore and reaction chambers are housed in a copper block which was heated with cartridge heaters (not shown in Figure 1) embedded in the copper block, and the temperature of the block and reaction chamber was determined with the thermocouple (TC).

(b) **Kinetics of Exchange Reactions.** Some experiments were performed in order to determine whether the ligand exchange reactions, eq 3, when proceeding in the exergonic, forward directions are near collision rates. When this is the case, the equilibria can be expected to establish rapidly, and the equilibria determinations are relatively straightforward.

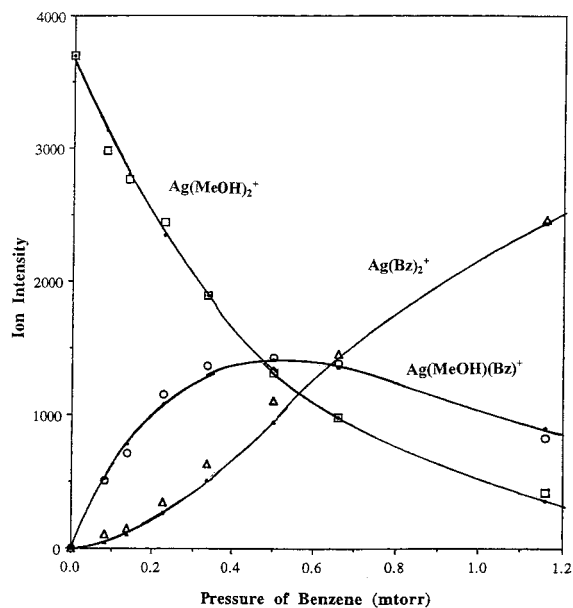


Figure 2. Observed ion intensities (ion counts per second) when $\text{Ag}(\text{MeOH})_2^+$ ions produced by the electro spray are drifted through reaction chamber RC (see Figure 1). Reagent gas in RC is 10 Torr of N_2 bath gas and benzene at partial pressures given on the horizontal axis. Ion intensity changes of $\text{Ag}(\text{MeOH})_2^+$ (\square), $\text{Ag}(\text{MeOH})(\text{Bz})^+$ (\circ), and $\text{Ag}(\text{Bz})_2^+$ (\triangle), are due to consecutive reactions: $\text{Ag}(\text{MeOH})_2^+ + \text{Bz} = \text{Ag}(\text{MeOH})(\text{Bz})^+ + \text{MeOH}$ and $\text{Ag}(\text{MeOH})(\text{Bz})^+ + \text{Bz} = \text{Ag}(\text{Bz})_2^+ + \text{MeOH}$. Full curves connecting experimental points are fits of the experimental points based on the theoretical rate equations for consecutive reactions.

The predominant ion species observed from electro spray of AgNO_3 in methanol solutions when pure N_2 gas was passed through the reaction chamber (see Figure 1), at 120 °C were $\text{Ag}(\text{MeOH})_2^+$ ions. The kinetic stage of the exchange reactions was observed by passing a reagent gas mixture through the reaction chamber which in addition to the N_2 contained a given ligand vapor at known pressures in the range 0–2 mTorr. Ion intensities observed under such conditions when the vapor was benzene are shown in Figure 2. The ion intensities follow the characteristic shapes expected for first-order consecutive reactions proceeding only in the forward direction. The reactions are first order because the concentration of the neutral benzene is many orders of magnitude higher than the ion concentration. The rate constant for reaction 3, eq 3a, where $\text{A} = \text{CH}_3\text{OH}$ and $\text{B} = \text{benzene}$, can be obtained by plotting the logarithm of the intensity of AgA_2^+ versus the partial pressure of benzene. Such a plot is shown in Figure 3. The rate constant is obtained with the equation

$$\ln \frac{I(\text{AgA}_2^+)}{I_0(\text{AgA}_2^+)} = -kt[\text{B}] \quad (6)$$

after converting the pressure to concentration $[\text{B}]$, where t , the residence time of the ion in the reaction chamber, is constant and the concentration of B is the variable. The residence time of the drifting ions through the reaction chamber was obtained by making kinetic determinations analogous to those shown in Figure 3 but for reactions with known rate constants. Thus, the known rate constant¹⁵ for the reaction $\text{H}_3\text{O}^+(\text{H}_2\text{O})_n + \text{CH}_3\text{COCH}_3 \rightarrow (\text{HCH}_3\text{COCH}_3)^+(\text{H}_2\text{O})_x + (\text{H}_2\text{O})_y$, where $n = 2$ and $n = 3$ equals $k = 3 \times 10^{-9}$ ($\text{cm}^3 \text{ molecule}^{-1} \text{ s}^{-1}$), led to an ion residence time $t = 113 \mu\text{s}$, while the analogous reaction involving methanol rather than acetone led to $t = 124 \mu\text{s}$. These

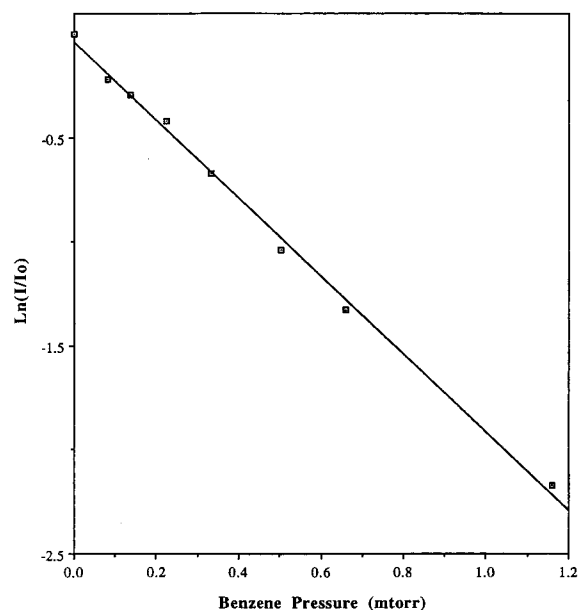


Figure 3. Logarithmic plot of the intensity changes of $\text{Ag}(\text{MeOH})_2^+$ ion with increasing pressure of benzene in reaction chamber. The intensity decreases due to the reaction $\text{Ag}(\text{MeOH})_2^+ + \text{Bz} = \text{Ag}(\text{MeOH})(\text{Bz})^+ + \text{MeOH}$. The slope of the straight line obtained is equal to the product of the rate constant k and the constant reaction time t ; see eq 6.

TABLE 1: Rate Constants for the Reaction $\text{Ag}^+(\text{MeOH})_2^+ + \text{L} = \text{Ag}^+(\text{MeOH})\text{L} + \text{MeOH}$ at 393 K^a

reactant L	k_{exp}^b	$k_{\text{ado}}^{b,c}$	$k_{\text{exp}}/k_{\text{ado}}$
ammonia	5×10^{-10}	1.5×10^{-9}	0.3
benzene	7×10^{-10}	1.02×10^{-9}	0.7
acetone	9×10^{-10}	1.7×10^{-9}	0.5
DMSO	1×10^{-9}	1.9×10^{-9}	0.6

^a Data evaluated from Arrhenius plots; see Figure 3. ^b k in units of $\text{cm}^3 \text{ molecule}^{-1} \text{ s}^{-1}$, data obtained from plots analogous to plot shown in Figure 5. Ion residence time $t = 110 \mu\text{s}$ was used. ^c Collision rates evaluated with the ADO theory equations.¹⁶

residence times are close to an estimated value of $t \approx 100 \mu\text{s}$, obtained previously¹⁰ which was based on expected ion drift velocities in the imposed ion drift field in a reaction chamber with conditions very similar to the present ones.

Rate constants for several exchange reactions are summarized in Table 1. The experimental rate constants are compared with collision rate values based on the average dipole orientation (ADO) theory.¹⁶ The experimental rates are found to be close to, but somewhat smaller than, the collision rates. On the average $k_{\text{exp}}/k_{\text{ADO}} \approx 0.5$. It should be noted that the present rate measurements cannot be considered to be of high accuracy. The experimental arrangement used was developed for equilibrium rather than rate measurements. Therefore, we can state with certainty only that the experimental rates are close and probably somewhat smaller than the collision rates. The results clearly demonstrate that the rates are very fast, thus suitable for equilibrium measurements.

The rate constant k_{3b} for the exchange of the second ligand (see eq 3b) can be determined by fitting the observed intensities (see Figure 2) to the theoretical rate equations for the consecutive reactions 3a and 3b which are irreversible when $-\Delta G^\circ_3$ is big as in the case in Figure 3. Such a fit is shown in Figure 2 where $\text{B} = \text{benzene}$. The value obtained is $k_{3b} = 0.94k_{3a}$, i.e., $k_{3b} = 6.6 \times 10^{-10} \text{ cm}^3 \text{ molecule}^{-1} \text{ s}^{-1}$ (see Table 1).

The mass spectrum showing the ions observed in a given run used for the determination of the kinetics where $\text{A} = \text{MeOH}$

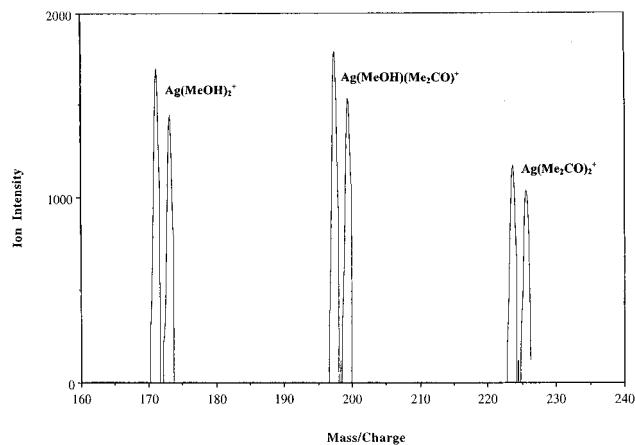


Figure 4. Mass spectra observed in rate constant measurements involving $\text{Ag}(\text{MeOH})_2^+$ and Me_2CO . The spectra are very clean. Essentially only the reactant ions are present.

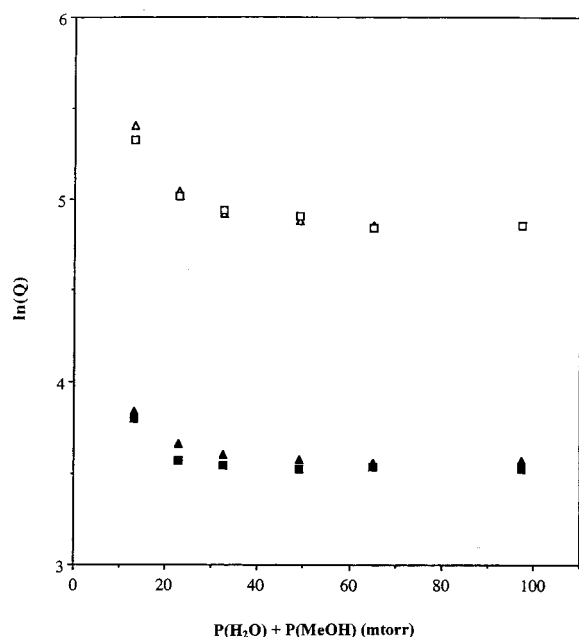


Figure 5. Achievement of equilibrium plot. $\text{Ag}(\text{MeOH})_2^+$ is supplied to reaction chamber which contains H_2O and MeOH at a constant partial pressure ratio. $P_{\text{H}_2\text{O}}/P_{\text{MeOH}} = 33.7$ (\square, \blacksquare); $P_{\text{H}_2\text{O}}/P_{\text{MeOH}} = 22.5$ ($\triangle, \blacktriangle$). Vertical axis gives values of equilibrium coefficients Q for reactions $\text{Ag}(\text{H}_2\text{O})_2^+ + \text{MeOH} = \text{Ag}(\text{H}_2\text{O})(\text{MeOH})^+ + \text{H}_2\text{O}$, upper curve with open symbols, and $\text{Ag}(\text{H}_2\text{O})(\text{MeOH})^+ + \text{MeOH} = \text{Ag}(\text{MeOH})_2^+ + \text{H}_2\text{O}$, lower curve with full symbols. As the total pressure of the two reagent gases is increased, the equilibrium quotients become constant, i.e., they become equal to the equilibrium constants K .

and $\text{B} = \text{acetone}$ is shown in Figure 4. It will be noticed that essentially the only ions observed are the ions AgA_2^+ , AgAB^+ , and AgB_2^+ , which are the ions expected for the reaction system eq 3; i.e., the mass spectra are very “clean”, and there is no interference from extraneous ionic species. Such clean spectra were generally obtained in both the kinetic and equilibrium measurements.

(c) Results from Measurements of the Equilibria. The kinetic investigations in the preceding section indicated that the equilibria would be observed at ligand gas pressure considerably in excess of 2 mTorr. The equilibria 3 were determined by using ligand pressures extending up to 100 mTorr. Results illustrating the procedure used are shown in Figures 5–7. The equilibrium quotients Q_{3a} and Q_{3b} corresponding to the equi-

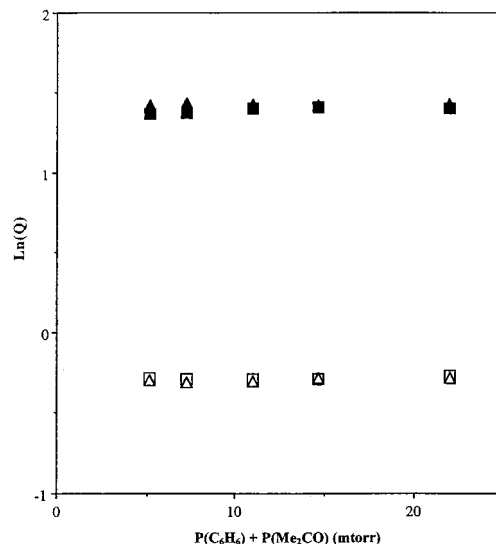


Figure 6. Achievement of equilibrium plot for reactions $\text{Ag}(\text{Bz})_2^+ + \text{Me}_2\text{CO} = \text{Ag}(\text{Bz})(\text{Me}_2\text{CO}) + \text{Bz}$, upper plot and $\text{Ag}(\text{Bz})(\text{Me}_2\text{CO})^+ + \text{Me}_2\text{CO} = \text{Ag}(\text{Me}_2\text{CO})_2^+ + \text{Bz}$, lower plot. Equilibrium is reached faster than was the case in Figure 5 because affinities of two reactants to Ag^+ are nearly equal. (\square, \blacksquare) $P(\text{Bz})/P(\text{Me}_2\text{CO}) = 1.22$; ($\triangle, \blacktriangle$) $P(\text{Bz})/P(\text{MeOH}) = 0.61$.

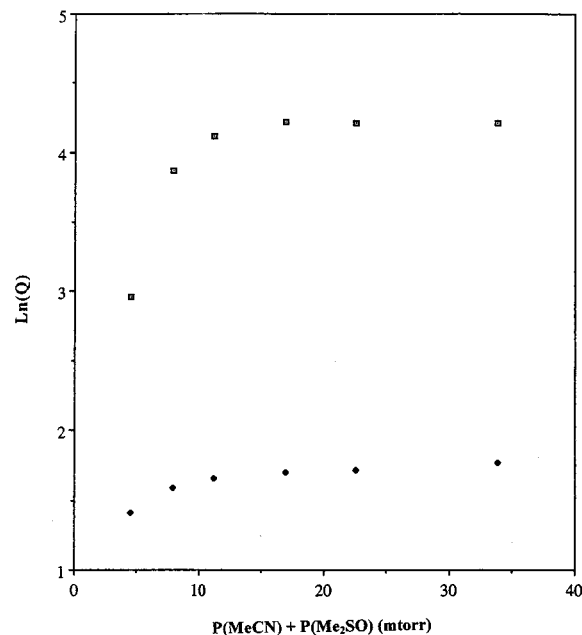


Figure 7. Achievement of equilibrium plot for reactions $\text{Ag}(\text{MeCN})_2^+ + \text{Me}_2\text{SO} = \text{Ag}(\text{MeCN})(\text{Me}_2\text{SO})^+ + \text{MeCN}$, upper plot, and $\text{Ag}(\text{MeCN})(\text{Me}_2\text{SO})^+ + \text{Me}_2\text{SO} = \text{Ag}(\text{Me}_2\text{SO})_2^+ + \text{MeCN}$, lower plot. Constant partial pressure ratio $P_{\text{MeCN}}/P_{\text{Me}_2\text{SO}} = 13.6$. Equilibrium quotient Q becomes constant only after the total pressure is equal to ~ 20 mTorr. At this point $P_{\text{Me}_2\text{SO}} \approx 2$ mTorr, which is a pressure just sufficient for the completion of the kinetic stage; see Figure 2.

librium constant expressions:

$$K_{3a} = \frac{I(\text{AgAB}^+)P_B}{I(\text{AgA}_2^+)P_A} \quad K_{3b} = \frac{I(\text{AgB}_2^+)P_B}{I(\text{AgAB}^+)P_A} \quad (7)$$

were determined from the observed ion intensities when a reaction mixture containing a given *constant* ratio of ligand partial pressures P_B/P_A flowed through the reaction chamber. The known partial pressure ratio was obtained by injecting with a motor-driven microsyringe into the heated nitrogen gas flow

a solution containing the weighed ratio of the two neat ligands. The pressure plotted on the horizontal axis corresponds to the sum of the partial pressures of the two ligands. On the basis of preliminary experiments, the ligand that led to weaker bonding was determined, and then in the final measurement the pressure of that ligand was set higher so as to obtain, at equilibrium, ion intensities that did not differ by very large factors. As the pressure is increased, the system should reach equilibrium; i.e.; the equilibrium quotients should become invariant with pressure and equal to the equilibrium constant. To check that equilibrium is truly achieved, experiments with different constant P_B/P_A ratios can be used, and these should lead to the same equilibrium constant when the equilibrium is reached (see Figures 5–7).

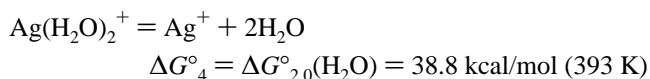
The plots shown in Figures 5–7 illustrate three typical cases. The exchange reaction, eq 3, in Figure 5 involves $A = \text{MeOH}$ and $B = \text{H}_2\text{O}$. Since the initial ions entering the reaction chamber are $\text{Ag}(\text{MeOH})_2^+$, the observed coefficient Q at low H_2O pressures where equilibrium has not yet been reached is higher than the equilibrium constant. The results shown in Figure 6 are for $A = \text{benzene}$ and $B = \text{acetone}$. These two ligands lead to similar bonding and are used at near equal pressure. Both ligands bond much more strongly than methanol. As the pressure of the ligands is increased, A and B rapidly displace the methanol from the original $\text{Ag}(\text{MeOH})_2^+$ ions. The observed equilibrium quotient does not show large changes with increasing total pressure. The experiment on which Figure 7 is based involves $A = \text{MeCN}$ and $B = \text{Me}_2\text{SO}$. B bonds more strongly and is used at a much lower concentration. At low total pressure, A which is present at much higher partial pressure replaces rapidly the MeOH . The quotient Q is initially smaller than the equilibrium constant K because the partial pressure of $B = \text{Me}_2\text{SO}$ is very low and the Me_2SO reaction is still in the kinetic stage. At a total ligand pressure of 20 mTorr, there is some 2 mTorr of Me_2SO present. This is sufficient for the completion of the kinetic stage, and the reaction gradually moves into the equilibrium stage.

The equilibria eq 3 were determined at 120 °C (393 K). At this temperature, the AgL_2^+ species were generally the major ions. At lower temperatures AgL_3^+ and AgL_n^+ where $n > 3$ become dominant.¹⁷

Results and Discussion

(a) Experimental Results and Thermochemical Data Obtained. The free energy changes ΔG_{3a}° , ΔG_{3b}° , and ΔG_3° for reactions 3 obtained from the equilibrium measurements at 393 K, described in the preceding section, are given in Table 2. Notable is the lower exoergicity of reaction 3b relative to reaction 3a. In cases where the total exoergicity of reaction 3 is relatively small, reaction 3b often becomes endoergic.

A scale of ΔG_3° values starting with $\text{Ag}(\text{H}_2\text{O})_2^+$ was obtained on the basis of these data (see Figure 8). The scale was calibrated to the free energy change for the reaction 4:



from the sum of the values $\Delta G_{1,0}^\circ$ and $\Delta G_{2,1}^\circ$ determined by Holland and Castleman⁵ by measurements of association equilibria. The absolute values ΔG_5° for the general reaction eq 5

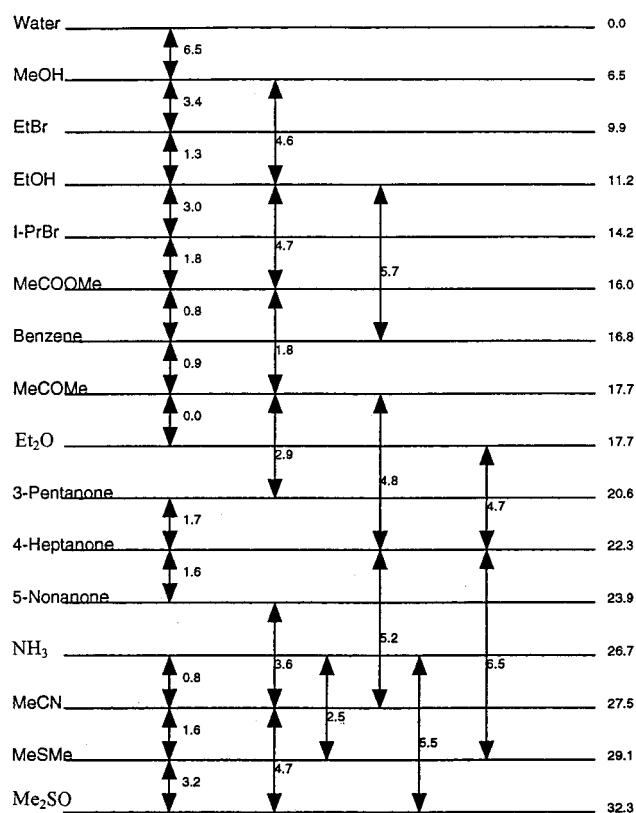
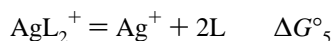


Figure 8. Scale of ΔG_3° values for the exchange equilibria $\text{AgA}_2^+ + 2\text{B} = \text{AgB}_2^+ + 2\text{A}$, determined at 393 K. Double arrows indicate ΔG_3° values of actual determinations. Some redundant determinations provide cross checks for values obtained.

TABLE 2: Free Energy Changes for Ligand Exchange Reactions, Eq 3

A/B	ΔG° at 393 K (kcal/mol)		
	AA → AB	AB → BB	AA → BB
H ₂ O/MeOH	3.8	2.7	6.5
MeOH/EtBr	2.2	1.2	3.4
MeOH/EtOH	2.8	1.8	4.6
EtBr/EtOH	1.1	0.2	1.4
EtOH/ <i>i</i> -PrBr	2.0	1.0	3.0
EtOH/MeCOOMe	3.0	1.7	4.7
EtOH/C ₆ H ₆	3.6	2.1	5.7
<i>i</i> -PrBr/MeCOOMe	1.5	0.3	1.8
MeCOOMe/C ₆ H ₆	1.1	-0.3	0.8
C ₆ H ₆ /MeCOMe	1.1	-0.2	0.9
MeCOMe/MeCOMe	1.4	0.4	1.8
MeCOMe/EtOEt	0.5	-0.5	0.0
MeCOMe/3-pentanone	1.8	1.1	2.9
MeCOMe/4-heptanone	3.0	1.8	4.8
EtOEt/4-heptanone	2.8	1.9	4.7
3-pentanone/4-heptanone	1.3	0.4	1.7
4-heptanone/5-nonanone	1.3	0.3	1.7
4-heptanone/MeCN	3.0	2.2	5.2
4-heptanone/MeSMe	4.3	2.2	6.5
5-nonanone/MeCN	2.1	1.5	3.7
NH ₃ /MeCN	0.9	-0.1	0.9
NH ₃ /MeSMe	1.9	0.6	2.4
NH ₃ /Me ₂ SO	3.9	1.6	5.5
MeCN/MeSMe	1.6	0.0	1.5
MeCN/Me ₂ SO	3.3	1.4	4.7
MeSMe/Me ₂ SO	3.2	0.0	3.3

obtained from this calibration of the relative scale (Figure 8) are given in Table 3.

To obtain estimates for the free energy changes at 298 K and to obtain also enthalpy changes $\Delta H_5^\circ(\text{L})$, the entropy changes ΔS_5° were evaluated from theory. The vibrational

TABLE 3: Thermochemical Data for the Reaction $\text{Ag(L)}_2^+ = \text{Ag}^+ + 2\text{L}$

L	ΔG_{393}° ^a	ΔG_{298}° ^b	ΔS° (cal/(K mol)) ^c	ΔH° (kcal/mol) ^d	η (L) ^f
H ₂ O	(38.8) ^e	43.9 ^e	(51) ^e 45	(58.7) ^e 56.5	9
MeOH	45.3	50.0	49	64.6	~7.5
EtBr	48.7	52.3	38	63.6	
EtOH	50.1	55.1	53	70.9	
<i>i</i> -PrBr	53.0	56.4	36	67.1	
MeCOOMe	54.8	59.2	47	73.3	
C ₆ H ₆	55.6	58.6	32	68.2	5.3
MeCOMe	56.5	60.1	38	71.4	5.6
EtOEt	56.5	61.8	56	78.5	
3-pentanone	59.5				
4-heptanone	61.2				
5-nonanone	62.8				
NH ₃	65.6	70.4	51	85.6	8.0
MeCN	66.5	70.8	46	84.5	7.5
MeSMe	68.0	72.4	47	86.4	~6
Me ₂ SO	70.9				

^a Experimental free energy change at 393 K determined in present work, unless otherwise noted. Estimated error ± 1.0 kcal/mol for relative values and ± 1.5 kcal/mol for absolute values. ^b Free energy change at 298 K evaluated from ΔG_{393}° and ΔS° . Estimated error ± 1 kcal/mol relative values, ± 2 kcal/mol absolute values. ^c Entropy change evaluated from vibrational, rotational, and translational entropies of reactants. Estimated error ± 6 cal/(K mol). ^d Enthalpy change evaluated from ΔG° values and ΔS° . Estimated error ± 3 kcal/mol for absolute values. ^e Experimental values obtained by Holland and Castleman.⁵ Errors given ± 2.2 kcal/mol for ΔH° and ± 3.4 cal/(K mol) for ΔS° . ^f Value for absolute hardness η of ligand L obtained with equation $\eta \approx (I - A)/2$, by Pearson,^{2d} see also Perason et al.,^{2c,e,f} where I is the ionization energy and A is the electron affinity of the ligand L.

TABLE 4: Calculated Entropies for Reactants^a L, Ag^+ , and AgL_2^+

L	S_{298}° (L) (cal/(K mol))	S_{298}° (AgL_2) (cal/(K mol))
H ₂ O	45.1	(45.1) ^b 84.9
MeOH	56.6	(57.3) 104.6
EtBr	68.1	(68.7) 138.6
EtOH	64.1	(67.5) 114.7
MeCOOMe	75.6	144.2
C ₆ H ₆	65.1	(64.3) 138.1
MeCOMe	71.1	(70.5) 144.0
EtOEt	79.5	(81.9) 142.6
NH ₃	48.2	(46.0) 86.0
MeCN	59.3	(58.2) 112.1
MeSMe	69.6	(68.3) 131.8

^a The entropy of Ag^+ , $S_{298}^\circ(\text{Ag}^+) = 39.9$ cal/(K mol). ^b Experimental values from ref 18.

frequencies of the reactants L and AgL_2 were obtained from ab initio calculations using HF/3-21G* basis sets of Gaussian 94. From these the vibrational entropy values at 298 K S_{vib}° were obtained. The rotational entropies, S_{rot}° were obtained from the theoretically evaluated moments of inertia while the translational entropies S_{trans}° were obtained with the Sackur–Tetrode equation. The resulting entropy values $S^\circ(\text{L})$ and $S^\circ(\text{AgL}_2^+)$ are given in Table 4. From these values, the entropy change ΔS_5° was evaluated at 298 and 393 K. The ΔS_5° values at 393 K were found to be within 1 cal/(K mol) of the 298 K values. Therefore, only the ΔS_5° at 298 K are given in Table 3. ΔG_5° values at 298 K obtained from the experimental ΔG_5° at 383 K were obtained from the relationship $\Delta G_{T_2}^\circ = \Delta G_{T_1}^\circ + \Delta S(T_2 - T_1)$, while ΔH_5° values were obtained from $\Delta H = \Delta G + T\Delta S$. These results are given in Table 3.

It is well-known that ab initio calculations with small basis sets such as 3-21G* and without electron correlation correction provide only poor estimates for the binding energies. On the other hand, the results for the vibrational frequencies are much

better.¹⁸ As a rule, small basis set calculations predict frequencies that are too high and can be brought into agreement¹⁸ with experimental or high-level calculation determined frequencies by multiplying with a factor of ~ 0.8 . We have not applied this factor to the evaluation of the ΔS_5° values given in Table 3. When this factor was applied, ΔS_5° values lower by some 6 cal/(K mol) were obtained while the ΔH_5° values decreased by ~ 2 kcal/mol. The correction factor of 0.8 was proposed¹⁸ largely on the basis of the high vibrational frequencies, which are much more numerous than the low frequencies $\bar{\nu} < 600$ cm^{-1} . However, it is the low frequencies that have a major effect on the S_{vib}° values. The correction factor 0.8 may not be suitable for the low frequencies which make the major contribution to ΔS . For this reason we have used the frequencies without correction. The changes of ΔS_5° (6 cal/(K mol)), ΔH_5° (2 kcal/mol), and ΔG_5° ($T = 298$ K) (0.7 kcal/mol) when the factors 1 and 0.8 are applied to the frequencies can be used to estimate the error introduced by the uncertainty in the 3-21G* predicted frequencies. Experimentally determined entropies¹⁹ for the ligands L are given in Table 4. On comparing these with the theoretically predicted values, one finds very good agreements—the differences are generally less than 1 cal/(K mol). However the error in the calculated entropies for AgL_2^+ may be considerably bigger since we do not know how well the HF/3-21G* accounts for the frequencies in AgL_2^+ . It is this concern that led to the choice of the rather large uncertainty of 6 cal/(K mol) for ΔS_5° . A comparison between the ΔS_5° values for L = H₂O, 45 ± 6 cal/(K mol) (calculated) and 51 ± 3.4 cal/(K mol), (experimental, Holland and Castleman⁵), shows that the results fall within the estimated error limits.

The present determination of the entropy changes ΔS_5° from the theoretically evaluated reactant entropies is in principle less satisfactory than an evaluation based on measurements of the temperature dependence of the equilibria 3 and determinations of ΔS_3° by means of van't Hoff plots. The absolute ΔS_5° values could then be obtained by calibration to ΔS_4° obtained by Holland and Castleman.⁵ However, ΔS_3° values obtained from temperature dependence measurements are reliable only if a relatively wide temperature range is used in each determination. The reaction chamber in the present apparatus cannot be heated above 480 K due to the cryopumping used. It was felt that this limited temperature range would not lead to entropy determinations for all reactions which are significantly better than the theoretically evaluated ΔS_5° values. Entropies evaluated with limited ab initio basis sets or semiempirical methods have been used with some success by other groups.^{6b,c}

(b) Discussion of Thermochemical Data for the AgL_2^+ Complexes. Theoretical studies by Bauschlicher et al.^{13,14} and experimental determinations^{5–7,18,19} have shown that transition-metal complexes ML_n^+ like CuL_n^+ and AgL_n^+ , have strong and nearly equal bonds for $\text{M}^+ - \text{L}$ and $\text{ML}^+ - \text{L}$. The $\Delta H_{1,0}^\circ$ and $\Delta H_{2,1}^\circ$ are high and nearly equal, while $\Delta H_{3,2}^\circ$, $\Delta H_{4,3}^\circ$, etc., are much smaller and decrease as n , $n - 1$ increases. For example, the values for $\text{Ag}(\text{H}_2\text{O})_n^+$ of Holland and Castleman⁵ in kcal/mol are $\Delta H_{1,0}^\circ = 33.3$, $\Delta H_{2,1}^\circ = 25.4$, $\Delta H_{3,2}^\circ = 15.0$, and $\Delta H_{4,3}^\circ = 14.9$, while for $\text{Cu}(\text{H}_2\text{O})_n^+$, Magnera et al.²⁰ provide the values 35, 39, 17, and 15. The transition-metal ion behavior is in contrast with bonding to the alkali ions such as Li^+ and Na^+ where the bond energies are highest for $\Delta H_{1,0}^\circ$ and decrease fairly regularly as n , $n - 1$ is increased.²¹ The features exhibited by the transition-metal ions can be rationalized on the basis of theoretical investigations.^{13,14} The bonding in the linear diligand complexes is strengthened by $\text{sd}\sigma$ orbital hybridization.^{13,14} The $\text{sd}\sigma$ hybridization reduces the electron

TABLE 5: Comparison between Bond Enthalpies for $\Delta H^\circ_{2,0}$ CuL_2^+ and AgL_2^+

L	CuL_2^+ (kcal/mol) ^a	L	AgL_2^+ (kcal/mol)
Me_2SO	111.7	Me_2SO	$\sim 87.4^b$
MeCN	107.6	Me_2S	86.3
NH_3	(104.4) ¹⁴	NH_3	85.5
Me_2S	100.7	MeCN	84.3

^a From ref 26. ^b Obtained from $\Delta G^\circ_{2,0}$ in Table 4 and estimated entropy, $\Delta S^\circ_{2,0} = 42$ cal/(K mol) based on the $\Delta S^\circ_{2,0}$ for acetone, see Table 3, arbitrarily augmented by 4 cal/(K mol).

charge density along the σ axis, and this allows the two ligands to approach the Ag^+ ion more closely. Most of the resulting bonding can be accounted on electrostatic grounds. The second ligand binding energy can be larger than the first, because both ligands benefit from reduced repulsion due to the $sd\sigma$ hybridization which occurs already with formation of the first bond; see ref 14. The large decrease in the third ligand binding energy has been attributed to the loss of $sd\sigma$ hybridization and to the increasing ligand repulsions as more ligands are added.¹⁴ Increasing ligand repulsion as the number of ligands increases is the major effect occurring for the alkali ion–ligand complexes whose binding energies decrease regularly starting already with the second ligand.

While it would have been desirable to have the individual values such as $\Delta H^\circ_{1,0}$ and $\Delta H^\circ_{2,1}$ for the AgL_2^+ complexes, the present results (Table 3) which provide only the sum of the two values are still of significant interest because in general $\Delta H^\circ_{1,0}$ and $\Delta H^\circ_{2,1}$ are expected to be quite close. Therefore, the values in Table 3 provide a good overview of the changes of bonding in AgL_2^+ for different ligands L.

There are only a few numerical results from the literature with which the present data can be compared. Holland and Castleman⁵ were able to obtain $\Delta H^\circ_{2,1} = 36.9$ kcal/mol for the $\text{Ag}(\text{NH}_3)_n^+$ complex. On subtracting this value from the present result for $\Delta H^\circ_5 = \Delta H^\circ_{2,0} = 85.6$ kcal/mol (Table 3), one obtains $\Delta H^\circ_{1,0} \approx 48.7$ kcal/mol; i.e., the $\Delta H^\circ_{1,0}$ is indicated to be considerably bigger as was the case for $L = \text{H}_2\text{O}$ (see above). For the benzene complex $\text{Ag}(\text{C}_6\text{H}_6)^+$, three $\Delta H^\circ_{1,0}$ values are available: 37.4,^{7b} 35,²² and 36.4 kcal/mol.¹³ Recent work by Dunbar and co-workers²³ reports binding energies of AgL_2^+ complexes based on an analysis of the competitive kinetics of radiative stabilization and autodissociation of excited AgL_2^+ complexes. For AgBz^+ they obtain $E_0 = 38.7$ kcal/mol while for AgBz_2^+ dissociating to AgBz^+ , the value is $E_0 \approx 34.6$ kcal/mol, for a total of 73.2 kcal/mol. The present value is $\Delta H^\circ_5 = 68.2$ kcal/mol. The agreement is fair. The second value of Dunbar (34.6 kcal/mol) may be somewhat high; see Tables 3 and 5 in ref 23. For $\text{Ag}(\text{Me}_2\text{CO})_2^+$ the sum of the two E_0 values obtained by Dunbar²³ is ~ 79 kcal/mol while the present data provide $\Delta H^\circ_4 = 71.4$ kcal/mol. Again, there is an indication²³ that the E_0 data may be somewhat high.

The data plot shown in Figure 9 provides a comparison between the bonding in the alkali ion–ligand complexes: LiL^+ , KL_2^+ and the transition-metal ion AgL_2^+ complexes. LiL^+ rather than LiL_2^+ were used because data for the LiL_2^+ complexes are not available. The binding energies for the AgL_2^+ complexes are considerably larger than those for the KL_2^+ complexes, as could be expected from the smaller crystallographic radius of Ag^+ ($R(\text{Ag}^+) = 1.26$ Å versus $R(\text{K}^+) = 1.33$ Å). Furthermore, because two ligand complexes are involved, the $sd\sigma$ hybridization which occurs only for Ag^+ decreases further the distance of approach of the two ligands, increasing thus the bonding in the AgL_2^+ complex.

The bond energies for the KL_2^+ complex are approximately

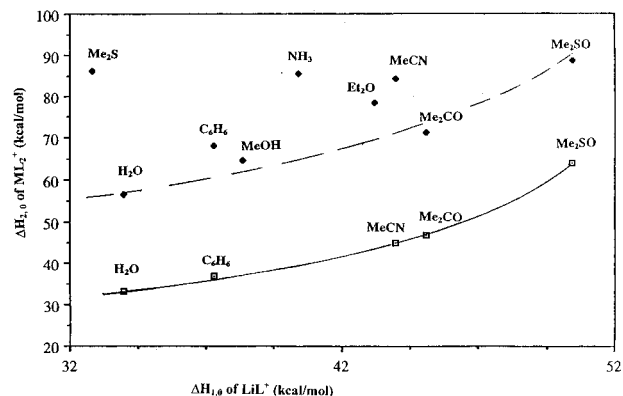


Figure 9. Comparison of binding enthalpies for $\text{AgL}_2^+ = \text{Ag}^+ + 2\text{L}$ and $\text{KL}_2^+ = \text{K}^+ + 2\text{L}$ shown on the vertical axis, with enthalpy for $\text{LiL}^+ = \text{Li}^+ + \text{L}$. The lower full curve shows good correlation between the alkali ion KL_2^+ and LiL^+ bond energies. The upper dashed curve shows that a correlation between the AgL_2^+ and LiL^+ values can be obtained only for the oxygen bases. The soft bases MeCN and particularly Me_2S show very large positive deviations, i.e. lead to relatively much stronger binding to Ag^+ . The bond energies of $\text{Ag}(\text{C}_6\text{H}_6)_2^+$ appear to be relatively only somewhat stronger, relative to that in $\text{K}^+(\text{C}_6\text{H}_6)_2$ where no d orbital participation is expected.

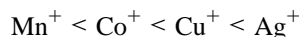
proportional to the LiL^+ data, as evident from Figure 9. On the other hand, a correlation is not present with the transition-metal AgL_2^+ data. The dashed curve shown indicates that an approximate correlation can be obtained if one selects only the oxygen ligands, i.e., H_2O , MeOH , Me_2CO , and Me_2SO . Relative to this correlation, the other ligands such as benzene, NH_3 , MeCN , and particularly Me_2S are seen to lead to a relatively stronger interaction with Ag^+ .

Of special interest is the very much stronger bonding of Me_2S in Ag^+ relative to the alkali ion complexes indicated by the data in Figure 9. Jones and Staley^{24,25} have reported comprehensive studies of ML_2^+ complexes where $\text{M}^+ = \text{Mn}^+$, Co^+ , and Cu^+ . These were based on ligand exchange equilibria determinations with an ion cyclotron resonance (ICR) mass spectrometer where the atomic metal ions were produced by laser pulses focused onto a wire of the given metal. These authors plotted the bond energies for the transition metals versus the bond energies of the LiL^+ complexes. These plots showed that the “soft” bases² MeSH and EtSH bond more strongly to the transition metals when compared with the harder oxygen bases. This was in agreement with the HSAB principle since the transition-metal ions are softer acids than is Li^+ and should bond more strongly to soft bases. Furthermore, the relative preference for the mercaptans was found^{24,25} to increase in the order $\text{Mn}^+ < \text{Co}^+ < \text{Cu}^+$. Jones and Staley^{24,25} pointed out that this observation is also in agreement with the HSAB principle because the softness of the acids Mn^+ (d^6), Cu^+ (d^8), Cu^+ (d^{10}) is expected²⁶ to increase in this order, presumably due to the increasing number of d electrons and experimental evidence from reactions studied in solution.

Jones and Staley’s measurements of CuL_2^+ complexes involved mostly weaker bonding ligands. To extend the comparison from CuL_2^+ to AgL_2^+ and the present results, which involved stronger bonding ligands, we have measured ligand exchange equilibria using Cu^+ ions produced by electrospray and ligands used in the present work. The complete data from these determinations will be published.²⁷ Here we use only a limited set of data involving the strongest bonding complexes. The methodology used for the Cu^+ complexes was analogous to that used for Ag^+ . The entropies were calculated, and absolute values were obtained by calibrating to the theoretical

value for $\text{Cu}(\text{NH}_3)_2^+ \rightarrow \text{Cu}^+ + 2\text{NH}_3$, $E_0 = 104.4$ kcal/mol, obtained by Bauschlicher et al.¹⁴ The relevant values²⁷ for CuL_2^+ and AgL_2^+ are shown in Table 5.

The data in Table 5 clearly show that the relative bond strength for Me_2S increases significantly from CuL_2^+ to AgL_2^+ . Thus, Me_2S is the most weakly bonded ligand to Cu^+ but moves to second place for Ag^+ . Combining this result with the data of Staley,^{24,25} one obtains the prediction that the relative bond strength in ML_2^+ for soft bases such as MeSH , Et_2SH and Me_2S increase in the order



i.e., with increasing softness of the Lewis acid, as expected from the HSAB principle.

While the bond energies for CuL_2^+ and AgL_2^+ where $\text{L} = \text{Me}_2\text{S}$ are in qualitative agreement with the HSAB principle, an examination of the relative bond energy values for some other ligands shows that a simple dependence on the HSAB predictions is not present. The numerical values for the absolute hardness η of the ligands L determined by Pearson^{2d} with the equation $\eta \approx (I - A)/2$, where I and A are the ionization energy and the electron affinity of the ligand, are given in Table 3. A good correlation with the HSAB η values would be present if the bases with the smallest η values, i.e., the softest bases, showed the largest upward deviation in the curve for the AgL_2^+ bonds in Figure 9. The largest deviation was for Me_2S which is soft, $\eta = 6$ (Table 3). However, NH_3 ($\eta = 8$) and MeCN ($\eta = 7.5$) also show fairly large upward deviations even though their η values are relatively high. Jones and Staley in their gas-phase determinations²⁵ also found that NH_3 and MeCN bond relatively more strongly to the softer acids and designated these bases as soft and in the same group as Me_2S ; see for example Figure 6 in ref 25b. This work was done before the absolute scale of hardness was developed by Pearson^{2c-g} which assigns greater hardness to NH_3 and MeCN . Benzene ($\eta = 5.3$), which is the softest base (Table 3), shows only a very small upward deviation in Figure 9, while one should have observed a very large upward deviation. These difficulties indicate that the HSAB principle in its present form provides somewhat limited insights into the bonding of gas-phase ion–ligand complexes when bases of different kinds are present. Better agreement is observed when bases of the same kind are examined.² The lack of good correlation when bases of a different kind are compared is due to the fact that the soft–soft combination accounts only for one component of the bonding, yet other components also make significant contributions.^{2f} Thus, in the gas phase, interactions between the charge of the ion and the permanent dipole of the ligand, when a strong dipole is present, make large contributions to the bonding.²⁷

Fortunately, relatively good ab initio calculations for metal ions as complex as Cu^+ and Ag^+ and ligands such as H_2O , NH_3 , and C_6H_6 are now possible.^{13,14} For example, the observed relatively small increase in the bonding of the soft base C_6H_6 to the soft acid Ag^+ may be rationalized on the basis of results by Bauschlicher et al.,¹³ who have pointed out that the bonding in $\text{Cu}(\text{C}_6\text{H}_6)_2^+$ is strengthened by back-donation of d orbital electrons into the π^* orbitals of benzene. However, for $\text{Ag}(\text{C}_6\text{H}_6)_2^+$ this effect is much smaller due to orbital mismatch.¹³ Possibly, it is the smallness of this bond strengthening effect that leads to only a slight increase of the bonding in $\text{Ag}(\text{C}_6\text{H}_6)_2^+$. We hope that the availability of the present experimental data will stimulate further computational work.

The present findings have applications also in other areas. Studies of electrospray mass spectra by Siu and co-workers²⁸

have shown that peptides and proteins electrosprayed from a solution that contains Ag^+ ions show enhanced formation of Ag^+ adducts when methionine ($-\text{CH}_2-\text{CH}_2\text{SCH}_3$) residues are present. In the absence of methionine, the Ag^+ will be probably multiply coordinated to peptide carbonyl groups. Bonding data for dicoordination to Na^+ are available.²⁹ When one or a few methionine groups are present, there still will be many more peptide carbonyl groups. Therefore, enhanced adduct formation in the presence of methionine would be expected only if the interaction of Ag^+ with methionine is especially strong. Such strong interactions are predicted by the present data.

The solvation energies of Ag^+ , Cu^+ , and Cu^{2+} salts in liquid solvent mixtures of water and acetonitrile have been studied by Marcus.³⁰ The Ag^+ and Cu^+ ions were found to be preferentially solvated by MeCN while Cu^{2+} was preferentially solvated by H_2O . Marcus was unable to estimate the distribution of H_2O and MeCN in the first solvation shell of Ag^+ and Cu^+ , for dilute solutions of MeCN in H_2O . While the present data cannot provide quantitative information on this distribution, the enormous difference in solvation exothermicity $-\Delta G_{0,2}^\circ = -43.9$ kcal/mol, $\text{Ag}(\text{H}_2\text{O})_2^+$, and $\Delta G_{0,2}^\circ = -70.8$ kcal/mol, $\text{Ag}(\text{MeCN})_2^+$ (Table 3)—strongly suggests that at least two molecules of MeCN should be present in the first shell of these ions.

Acknowledgment. This work was supported by grants from the Canadian Natural Sciences and Engineering Research Council (NSERC).

References and Notes

- (1) (a) Russel, D. H., Ed. *Gas-Phase Inorganic Chemistry*; Plenum Press: New York, 1989. (b) Freiser, B. S., Ed. *Organometallic Ion Chemistry, Understanding Chemical Reactivity 15*; Kluwer Academic Publishers: Dordrecht, The Netherlands, 1996. (c) Freiser, B. S. *Acc. Chem. Res.* **1994**, *27*, 353.
- (2) (a) Bassolo, F.; Pearson, R. G. *Mechanism of Inorganic Reactions*, 2nd ed.; Wiley: New York, 1967; p 33ff. (b) Huheey, J. E. *Inorganic Chemistry*, 3rd ed.; Harper & Row: New York, 1983; p 312ff. (c) Parr, R. G.; Pearson, R. G. *J. Am. Chem. Soc.* **1983**, *105*, 7512. (d) Pearson, R. G. *Inorg. Chem.* **1988**, *27*, 734. (e) Pearson, R. G. *J. Am. Chem. Soc.* **1988**, *110*, 7684. (f) Pearson, R. G. *J. Org. Chem.* **1989**, *54*, 1423. (g) Pearson, R. G. *Inorg. Chim. Acta* **1995**, *240*, 93.
- (3) (a) Yamashita, M.; Fenn, J. B. *J. Phys. Chem.* **1984**, *88*, 4451. (b) Fenn, J. B.; Mann, M.; Meng, C. K.; Wong, S. F.; Whitehouse, C. M. *Science* **1985**, *246*, 64. (c) Kebarle, P.; Tang, L. *Anal. Chem.* **1993**, *64*, 272A.
- (4) Kebarle, P. *Annu. Rev. Phys. Chem.* **1977**, *28*, 445.
- (5) Holland, P. M.; Castleman, Jr., A. W. *J. Chem. Phys.* **1982**, *76*, 4195.
- (6) (a) Armentrout, P. B. Thermochemical measurements by guided beam mass spectrometry. In Adams, N.; Babcock, L. M., Eds. *Advances in Gas-Phase Ion Chemistry*; JAI Press: Greenwich, 1992; Vol. 1, p 83. (b) Dalleska, N. F.; Honma, K.; Armentrout, P. B. *J. Am. Chem. Soc.* **1993**, *115*, 12125. (c) Dalleska, N. F.; Honma, K.; Sunderlin, L. S.; Armentrout, P. B. *J. Am. Chem. Soc.* **1994**, *116*, 3519.
- (7) (a) Mayer, F.; Chen, Y. M.; Armentrout, P. B. *J. Am. Chem. Soc.* **1995**, *117*, 4071. (b) Chen, Y. M.; Armentrout, P. B. *Chem. Phys. Lett.* **1993**, *210*, 123.
- (8) Szulejko, J. E.; McMahon, T. B. *J. Am. Chem. Soc.* **1993**, *115*, 7839.
- (9) Taft, R. W.; Anvia, F.; Gal, J. F.; Walsh, S.; Capon, M.; Holmes, M. C.; Hosn, K.; Oloumi, G.; Vasanwala, R.; Yazdani, S. *Pure Appl. Chem.* **1990**, *62*, 17.
- (10) Klassen, J. S.; Blades, A. T.; Kebarle, P. *J. Phys. Chem.* **1995**, *99*, 15509.
- (11) Blades, A. T.; Klassen, J. S.; Kebarle, P. *J. Am. Chem. Soc.* **1996**, *118*, 12437.
- (12) (a) Blades, A. T.; Jayaweera, P.; Ikonomou, M. G.; Kebarle, P. *J. Chem. Phys.* **1990**, *92*, 5900. (b) Blades, A. T.; Jayaweera, P.; Ikonomou, M. G.; Kebarle, P. *Int. J. Mass Spectrom. Ion Processes* **1990**, *101*, 325; **1990**, *102*, 251. (c) Blades, A. T.; Klassen, J. S.; Kebarle, P. *J. Am. Chem. Soc.* **1995**, *117*, 10563. (d) Klassen, J. S.; Andersson, S. G.; Blades, A. T.; Kebarle, P. *J. Phys. Chem.* **1996**, *100*, 14218.

- (13) Bauschlicher, C. W.; Partridge, H.; Langhoff, S. R. *J. Phys. Chem.* **1992**, *96*, 3273.
- (14) Bauschlicher, C. W.; Langhoff, S. R.; Partridge, H. *J. Chem. Phys.* **1991**, *94*, 2068.
- (15) Bohme, D. K.; Mackay, G. I.; Tanner, S. D. *J. Am. Chem. Soc.* **1979**, *101*, 3724.
- (16) Su, T.; Bowers, M. T. *J. Mass Spectrom. Ion Processes* **1975**, *17*, 211.
- (17) When a bath gas is used at relatively high pressures, as is the case in the present experiments, one has the advantage of having ensured the thermalization of the ions; however, because the bath gas provides the third body required for the association kinetics, one has to contend with the presence of association reactions (see eq 1). With ICR and FTICR where very low gas pressures are used, $p < 10^{-6}$ Torr, association kinetics are extremely slow, and exchange equilibria can be determined in principle at any temperature so long as the free energy change of the reaction is small.
- (18) Sceger, D. M.; Korziniewsky, C.; Kowalchuk, W. *J. Phys. Chem.* **1991**, *95*, 68.
- (19) Stull, D. R.; Westrum, Jr., E. F.; Sinke, G. C. *The Chemical Thermodynamics of Organic Compounds*; John Wiley & Sons: New York, 1969.
- (20) (a) Magnera, T. F.; David, D. E.; Stulik, R. G.; Orth, R. G.; Jonkman, H. T.; Michl, J. *J. Am. Chem. Soc.* **1989**, *111*, 5036. (b) Martinelli, P. J.; Squires, R. R. *J. Am. Chem. Soc.* **1989**, *111*, 4101.
- (21) Dzidic, I.; Kebarle, P. *J. Phys. Chem.* **1970**, *74*, 1466.
- (22) McMahon, T. B. Unpublished result quoted by Bauschlicher et al.¹³
- (23) Yen-Peng, H.; Yu-Chuan, Y.; Klippenstein, J.; Dunbar, R. C. *J. Phys. Chem. A* **1997**, *101*, 3338.
- (24) Jones, R. W.; Staley, R. H. *J. Phys. Chem.* **1982**, *86*, 1387.
- (25) (a) Jones, R. W.; Staley, R. H. *J. Am. Chem. Soc.* **1982**, *104*, 1235, (b) 1238, (c) 2296.
- (26) The HSAB equations quantitatively predicting the hardness η of acids and bases^{2c-g} $\eta = (I - A)/2$, where I is the ionization energy and A the electron affinity of the acid or base, had not been developed at the time of the Jones and Staley^{24,25} publications. Actually, the order predicted by the quantitative equation for η of Co^+ ($\eta = 4.6$), Cu^+ ($\eta = 6.3$), and Ag^+ ($\eta = 6.96$)^{2d} predicts decreasing softness in the order Co^+ , Cu^+ , Ag^+ , which is the opposite of that assumed by Jones and Staley.²⁵ However, Pearson² has pointed out that the quantitative equation for η of ions does not work for many ions and given reasons for the failure of the equation.
- (27) Deng, H.; Kebarle, P. Binding Energies of Copper Ion-ligand Complexes CuL_2^+ , from Ligand Exchange Equilibria. *J. Am. Chem. Soc.*, submitted for publication.
- (28) Li, H.; Siu, M. K. W.; Guevremont, R.; LeBlanc, Y. J. C. *J. Am. Soc. Mass Spectrom.* **1997**, *8*, 781.
- (29) Klassen, J. S.; Anderson, S. G.; Blades, A. T. *J. Phys. Chem.* **1996**, *100*, 14218.
- (30) Marcus, Y. *J. Chem. Soc., Dalton Trans.* **1991**, 2265.